Frequency-dependent reduction of voltage-gated sodium current modulates retinal ganglion cell response rate to electrical stimulation

2011 J. Neural Eng. 8 066007

(http://iopscience.iop.org/1741-2552/8/6/066007)

J. Neural Eng. **8** (2011) 066007 (12pp) doi:10.1088/1741-2560/8/6/066007

Frequency-dependent reduction of voltage-gated sodium current modulates retinal ganglion cell response rate to electrical stimulation

David Tsai[1], John W Morley[2,3], Gregg J Suaning[1] and Nigel H Lovell[1,4]

[1] Graduate School of Biomedical Engineering, University of New South Wales, Sydney, NSW 2052, Australia
[2] School of Medicine, University of Western Sydney, Sydney, NSW 1797, Australia
[3] School of Medical Sciences, University of New South Wales, Sydney, NSW 2052, Australia

E-mail: N.Lovell@unsw.edu.au

Received 5 August 2011
Accepted for publication 27 September 2011
Published 26 October 2011
Online at stacks.iop.org/JNE/8/066007

Abstract

The ability to elicit visual percepts through electrical stimulation of the retina has prompted numerous investigations examining the feasibility of restoring sight to the blind with retinal implants. The therapeutic efficacy of these devices will be strongly influenced by their ability to elicit neural responses that approximate those of normal vision. Retinal ganglion cells (RGCs) can fire spikes at frequencies greater than 200 Hz when driven by light. However, several studies using isolated retinas have found a decline in RGC spiking response rate when these cells were stimulated at greater than 50 Hz. It is possible that the mechanism responsible for this decline also contributes to the frequency-dependent 'fading' of electrically evoked percepts recently reported in human patients. Using whole-cell patch clamp recordings of rabbit RGCs, we investigated the causes for the spiking response depression during direct subretinal stimulation of these cells at 50–200 Hz. The response depression was not caused by inhibition arising from the retinal network but, instead, by a stimulus-frequency-dependent decline of RGC voltage-gated sodium current. Under identical experimental conditions, however, RGCs were able to spike at high frequency when driven by light stimuli and intracellular depolarization. Based on these observations, we demonstrated a technique to prevent the spiking response depression.

(Some figures in this article are in colour only in the electronic version)

Introduction

There has been a long-standing interest in restoring sight to the blind. Many research groups have been developing implants that target neurons in the retina. These implants operate by activating the surviving neurons following the loss of photoreceptors due to conditions such as retinitis pigmentosa. Human trials over the last decade have demonstrated the ability of these retinal implants to elicit simple visual percepts such as bright light spots (Gerding *et al* 2002, Rizzo *et al* 2003, Gekeler *et al* 2006, Fujikado *et al* 2007, Greenwald *et al* 2009, Horsager *et al* 2011). When driven by laboratory visual stimuli and natural scenes, retinal ganglion cells (RGCs) are able to fire spikes at frequencies above 200 Hz (Meister 1999, Baccus 2007), and for some cells over 300 Hz under appropriate conditions (Zeck and Masland 2007). Thus, these high-frequency spike trains may be the fundamental coding blocks with which the retina conveys visual information (Berry *et al* 1997). To maximize the quality of electrically evoked percepts, retinal implants may need to activate these cells at

[4] Author to whom any correspondence should be addressed.

similar frequencies. However, several investigations using isolated retinas have found a decline in spiking response rate while electrically stimulating RGCs directly (as opposed to indirect responses of synaptic origin) at $\geqslant$50 Hz (Sekirnjak *et al* 2006, Tsai *et al* 2009). Similarly, others described failures to generate full action potentials (Cai *et al* 2011) and increasing RGC threshold (Freeman and Fried 2011) during repeated stimulation. Recent human clinical studies have reported a frequency-dependent 'fading' of electrically evoked percepts (Zrenner *et al* 2010, Christopher *et al* 2010). In some subjects, the percepts lasted for less than a second. While the reason(s) for the fading percepts is unknown, the spiking response depression observed in studies using isolated retinas suggests that retinal mechanisms could be responsible, at least in part, for the response fading. This is particularly plausible given studies demonstrating use-dependent inactivation of voltage-gated sodium channels (Debanne 2004), which is the primary mechanism behind RGC direct responses following electrical stimulation (Fried *et al* 2009).

In this study, we investigate the cause of RGC spiking response depression when these cells are electrically stimulated at $\geqslant$50 Hz. We found the effects of retinal network inhibition to be insignificant in suppressing RGC spiking probability during repetitive stimulation. The evoked RGC voltage-gated sodium current (I_{Na}), however, decreased exponentially. We then demonstrate that RGC spiking response rate decline was prevented by counteracting the decline of electrically evoked sodium current. Finally we show that under identical conditions, these RGCs were intrinsically capable of high-frequency repetitive spiking and did so when stimulated by light.

Methods

Preparation

All procedures were approved and monitored by the Animal Care and Ethics Committee at University of New South Wales. NZ White rabbits were anesthetized intramuscularly with ketamine (70 mg kg^{-1}) and xylazine (10 mg kg^{-1}), then euthanized with an intravenous overdose of pentobarbital. Inferior retinas, encompassing the visual streak, were isolated and kept in Ames' Medium supplemented with 1% penicillin/streptomycin and saturated with 95% O_2 and 5% CO_2 at room temperature. The retinas were kept under this condition in darkness for 1–12 h. Prior to recording, a piece of the retina was transferred RGC-side up to a fixed-stage upright microscope. The retinas were perfused continuously with equilibrated Ames' Medium warmed to 34–35 °C (pH 7.4) at ~5 mL min^{-1}.

Patch clamp electrophysiology

The RGCs were selected for recording by targeting cells with somatic diameter >10 μm and just beneath the inner limiting membrane (Vaney 1980). In most experiments, we also ascertained that the targeted cells were RGCs, and not displaced starburst amacrine cells, by epi-fluorescence microscopy of Alexa Fluor 488 (75 μM; Invitrogen) in the pipette solution. Furthermore, starburst amacrine cells in the adult rabbit retina do not fire somatic action potentials (Zhou and Fain 1996, Zheng *et al* 2004). Together, these rule out the possibility of contamination by amacrine cells. Current clamp electrodes were filled with (mM) 120 $KMeSO_4$, 10 KCl, 0.008 $CaCl_2$, 0.5 EGTA, 1 $MgCl_2$, 10 HEPES, 4 ATP-Na_2 and 0.5 GTP-Na_3, adjusted to pH 7.2 with KOH. Final pipette resistances were 2.5–5.0 MΩ. All chemicals were purchased from Sigma Aldrich. A 5 mV liquid junction potential correction has been applied for all results. For cell-attached recordings, the pipettes were filled with Ames' medium. A Multiclamp 700B (Molecular Devices) amplifier, Digidata 1440A (Molecular Devices) and custom-written software were used for data acquisition. Data were low-pass filtered at 10 kHz and digitized at 50 kHz. Current clamp series resistance was compensated with the bridge balance control. Voltage clamp series resistance was compensated by 33–50% at 5–7 kHz bandwidth.

Data were analyzed in pClamp 10 (Molecular Devices), Matlab 2009 (Mathworks Inc.), Minitab 15 (Minitab Inc.) and Prism 5.0a (GraphPad Software). The statistical significance level was set at 95% (two-tailed). Data are presented as the mean ± standard error of mean.

Pharmacology

The AMPA/kainate, NMDA, mGluR6, $GABA_{a/c}$ and glycine receptors were blocked with (in mM) 0.075 6-cyano-7-nitroquinoxaline-2,3-dione (CNQX), 0.06 (+)-MK 801 hydrogen maleate (MK-801), 0.02 L-(+)-2-amino-4-phosphonobutyric acid (L-AP4), 0.1 picrotoxin (pic) and 0.01 strychnine (stry), respectively. The blocking efficacy was ascertained by the lack of light-evoked RGC responses. Voltage-gated sodium channels were blocked with 0.5 μM tetrodotoxin (TTX). Calcium currents were non-selectively blocked with 250 μM $CdCl_2$. All drugs were bath-applied. All pharmacological agents were purchased from either Sigma Aldrich or Tocris Bioscience.

Electrical stimulation

We stimulated the isolated neural retinas at the photoreceptor side (subretinal stimulation). The stimuli were delivered via a single 40 × 40 μm^2 planar electrode in a multielectrode array (MEA; Ayanda Biosystems), with 60 platinum electrodes on a glass substrate and arranged in a square grid with 200 μm electrode center-to-center distance. The stimulus return was via eight distant electrodes at the MEA perimeter connected in parallel.

Symmetric, charge-balanced, constant-current, biphasic, rectangular pulses were generated from a custom-built stimulus generator. All biphasic pulses were cathodic-first and without inter-phase delay. Here, we defined the pulse amplitude and duration as the height and width, respectively, for one phase of the biphasic pulse. Each stimulus presentation was separated by at least a 1 s delay.

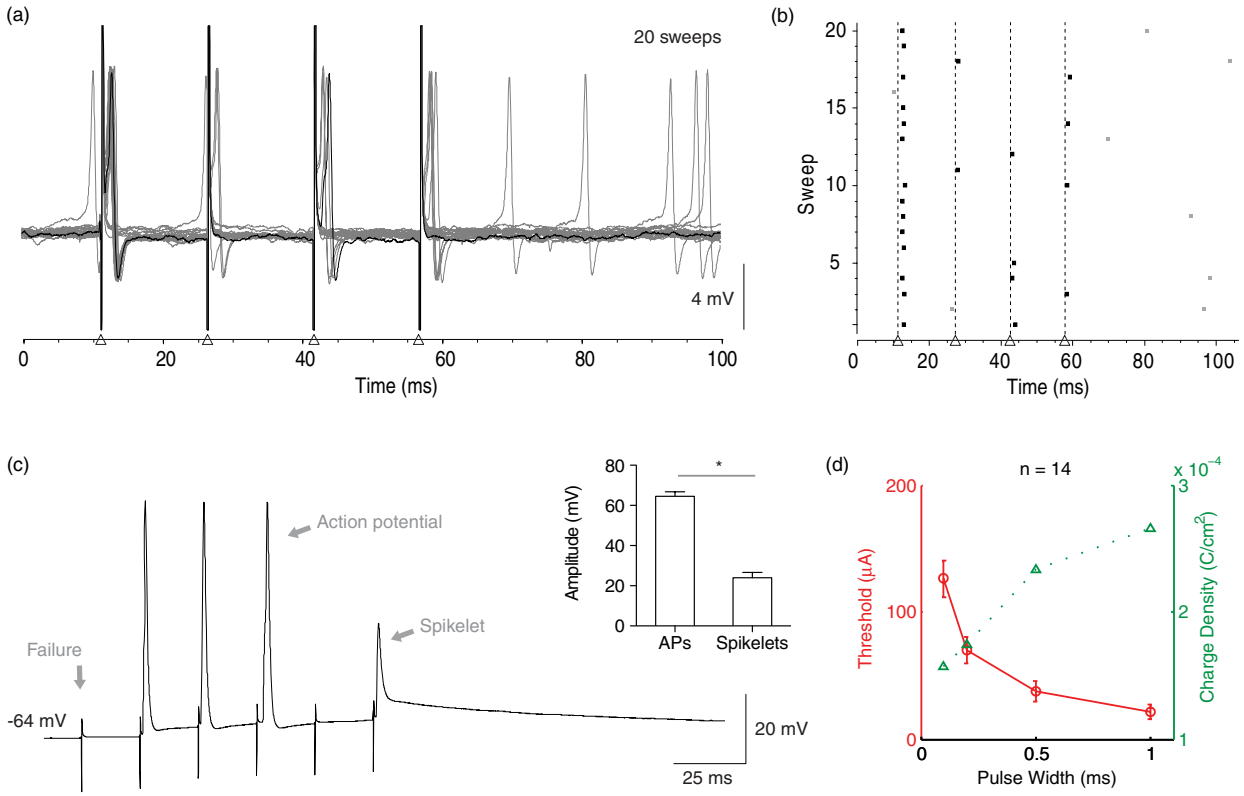

Figure 1. RCG spikes evoked by repetitive stimulation. (a) Superimposed cell-attached extracellular recordings of a RGC stimulated with a 66.6 Hz train consisting of four 100 μA 0.1 ms biphasic pulses. The stimulus delivery times are marked by the triangles. The spikes are easily distinguished from the stimulus artifacts (vertical lines). The first sweep is denoted in black. (b) Raster plot for the spikes in (a). Marked in black are the short-latency spikes due to direct RGC stimulation. (c) In some cells, stimulation occasionally evoked spikelets with amplitude much smaller than that of full action potentials ($p < 0.0001$, t-test, $n = 5$ cells). Spikelets were apparent during whole-cell current clamp recordings. The stimuli were 0.1 ms at 110 μA. (d) Mean threshold current (red) that elicited a direct RGC spike and the equivalent charge density values (green) for evoking direct RGC responses.

Measuring RGC response rate depression

We characterized RGC spiking response rate depression during repetitive, direct activation by stimulating the cells with a train of four identical biphasic pulses. We defined direct activation as RGC spiking responses ($\leqslant$2 ms latency) that are resistant to synaptic input blocking, as determined in a previous study (Tsai *et al* 2009). We note that varying direct activation latencies have been reported under different conditions and stimulation configurations (<0.7 ms in Fried *et al*; 0.35 ms in Sekirnjak *et al*; <7 ms in Ahuja *et al* 2008). For each RGC, we began by determining the stimulus threshold that evoked a direct RGC response in approximately 80% of trials (over 20 repetitions). All subsequent stimuli used this threshold current. Four pulse train frequencies were tested (50, 66.6, 100 and 200 Hz). For each frequency, we tested three pulse widths (0.1, 0.2 and 0.5 ms), for a total of 12 test combinations. To determine the mean spiking response rate for each stimulus of the pulse train, each combination was repeated at least ten times.

The I_{Na} decline rate during repetitive, direct RGC stimulation was determined analogously. Unlike the all-or-none action potentials, the evoked I_{Na} amplitude is stimulus-strength dependent. Thus, when measuring I_{Na}, we used stimuli that are close to the average RGC threshold values (figure 1(d)). We used six consecutive 0.1 ms pulses at three pulse train frequencies (50, 100 and 200 Hz). Finally, instead of counting spikes, whole-cell voltage clamp was used to measure the evoked I_{Na}. The calcium-mediated currents were blocked with 250 μM $CdCl_2$ in the perfusion bath. The mean evoked I_{Na} for each pulse was determined by repeating the same pulse train ten times. The I_{Na} reduction rate was described with a one-phase exponential decay equation:

$$I_n = (1 - \alpha) \times e^{-kn} + \alpha,$$

where I_n is the evoked I_{Na} for the nth pulse, relative to the I_{Na} for the first pulse ($n = 0$). Least-squares fitting was used to determine the parameters α and k, which are the exponential decay plateau limit and rate constant, respectively.

Light stimulation

RGCs were visualized with near-infrared (>820 nm) illumination. All recordings were performed under mesopic ambient lighting (~7 cd.sr.m^{-2}) with light-adapted retinas. A stationary light spot from a white light-emitting diode behind

a pinhole was focused onto the photoreceptor layer using the microscope's 40× objective lens (Nikon NIR APO 0.8 N.A). The spot covered a 160 μm diameter circular area. We took the soma as the center of the cell's receptive field. To characterize the response type (ON, OFF and ON-OFF) and the inter-spike intervals (ISIs) of light-evoked responses, we presented the cells with a 4 s light sequence consisting of ON-OFF-ON-OFF, each of 1 s duration. This was repeated five times with 5 s delay between presentations. The mean light-evoked ISIs were calculated by averaging the ISIs across the five repetitions. Only cells with a clearly defined response classification (ON, OFF and ON-OFF) were included for analysis. To calculate the mode for each ISI, we fitted the duration distribution data for each ISI with a log-normal probability density function (PDF):

$$f(x|\mu,\sigma) = \frac{1}{x\sigma\sqrt{2\pi}}\,\mathrm{e}^{\frac{-(\ln x-\mu)^2}{2\sigma^2}}.$$

The parameters (μ and σ) for each log-normal PDF were determined by maximum likelihood estimation (Matlab). In all cases, the goodness of fit was ascertained using the Anderson–Darling test (Stephens 1974; $p \geqslant 0.107$). Finally, the mode was then given by

$$\mathrm{e}^{\mu-\sigma^2}.$$

Results

Depression of RGC spiking responses during repeated stimulation

RGCs could be directly activated by extracellular electrical stimulation, eliciting spikes with latency $\leqslant$2 ms (Fried *et al* 2006, Sekirnjak *et al* 2006). Other neurons in the retinal network (e.g. bipolar cells and amacrine cells) could also be activated by electrical stimulation. However, these cells respond poorly to stimuli greater than a few Hz (Sekirnjak *et al* 2006, Jensen and Rizzo 2007, Ahuja *et al* 2008). Figure 1(a) shows 20 superimposed cell-attached recordings of a cell stimulated directly with a train of four 0.1 ms biphasic pulses at 66.6 Hz. The spiking response rate decreased from 70% following the first pulse to 10–20% for the subsequent pulses (figure 1(b)). In the following work, we investigated the mechanisms underlying the decrease in RGC spiking response rate during repetitive direct RGC stimulation.

Electrical stimulation occasionally failed to elicit a full action potential in some RGCs. Instead, it evoked a small-amplitude depolarization, which we will refer to as 'spikelets'. During whole-cell current clamp recordings, these spikelets were characteristically different from action potentials and complete elicitation failures (figure 1(c)). In five RGCs (one ON cell, two OFF cells and two ON-OFF cells; determined by light stimulation), where these responses were observed, the spikelet mean amplitude was significantly smaller than that of action potentials (64.6 $\pm$ 2.3 mV versus 24.0 $\pm$ 2.7 mV, $p < 0.0001$, t-test). Spikelets are known features of neurons in other CNS regions, for instance in hippocampal neurons (Spencer and Kandel 1961) and in inferior olive neurons (Llinas *et al* 1974). However, these were not conventional RGC action potentials evoked by intracellular depolarization (e.g. figure 7) and light stimulation (e.g. figure 8). Thus, in the responses described below, we excluded these spikelets from analysis. To facilitate comparison with existing studies, we also determined the thresholds and charge densities for eliciting direct RGC spikes across a range of pulse widths (figure 1(d)) with the present 40 μm × 40 μm subretinal electrodes.

RGC intrinsic properties underlie spiking response depression during repetitive direct stimulation

RGCs are capable of high-frequency spiking when driven by light. A number of previous prosthetic stimulation studies have observed a decline in RGC spiking response rate during repetitive direct stimulation at $\geqslant$50 Hz. Electrical stimuli could activate amacrine cells (Fried *et al* 2006, Margalit and Thoreson 2006), in addition to RGCs; thus, inhibition from these cells could potentially underlie the response depression. To test this hypothesis under a variety of stimulation configurations, we stimulated RGCs ($n = 10$) directly with a train of four identical biphasic pulses at four frequencies (50, 66.6, 100 and 200 Hz), and for each frequency at three pulse widths (0.1, 0.2 and 0.5 ms). We first stimulated RGCs under the control condition without the blockers (figure 2, red; left group). We then repeated the stimuli while blocking all presynaptic inputs (figure 2, green; right group). The differences in response rate across the four pulses were statistically significant, with or without blocking (0.1 ms: $p = 0.001$, 0.2 ms: $p = 0.0003$, 0.5 ms: $p < 0.0001$, repeated measure two-way ANOVA). More importantly, blocking the presynaptic inputs did not improve the RGC response rate during repetitive stimulation (0.1 ms: $p = 0.761$, 0.2 ms: $p = 0.271$, 0.5 ms: $p = 0.810$). These results suggest that inhibition from amacrine cells following electrical stimulation did not play a significant role in suppressing the response rate of directly activated RGCs, at least not for the stimulus duration used here.

Evoking I_{Na} with extracellular stimulation while voltage clamping RGCs at rest

Voltage-gated sodium channels play an important role in determining neuronal excitability during extracellular electrical stimulation. We therefore asked if these channels were responsible for the response depression observed during high-frequency stimulation. Whole-cell voltage clamp with simultaneous extracellular stimulation of presynaptic cells has been used extensively to study excitatory and inhibitory postsynaptic currents (EPSCs and IPSCs). Before quantifying the sodium current evoked by electrical stimulation, we began by verifying that the voltage clamp technique (clamping at resting potential) could also be applied to quantify RGC voltage-gated sodium current evoked by extracellular stimulation. When RGCs were clamped at rest ($n = 3$, $V_{\mathrm{hold}} = -65$ mV), electrical stimulation consistently evoked a single inward current with fast activation kinetics (figure 3(a), red trace, arrow). The mean peak current amplitude and latency (measured from the stimulus artifact

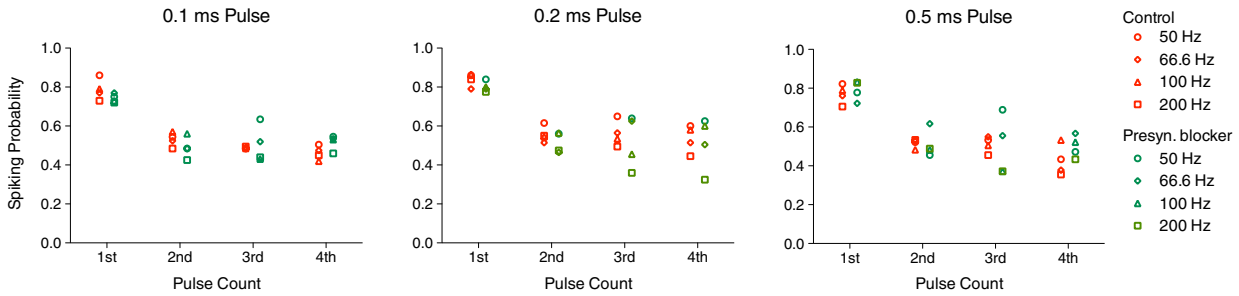

Figure 2. Blocking presynaptic inputs did not improve RGC spiking response rate during repetitive stimulation. Ten RGCs were stimulated with a train of four biphasic pulses (50–200 Hz, 0.1–0.5 ms pulse width), and the probability of eliciting a spike through direct activation of the RGCs was determined over ten trials. For both the control condition without the blockers (red; left group) and with presynaptic input blocked (green; right group; CNQX + MK-801 + L-AP4 + pic + stry), the decline in response rates was significant (0.1 ms: $p = 0.001$, 0.2 ms: $p = 0.0003$, 0.5 ms: $p < 0.0001$; repeated measure two-way ANOVA). However, blocking the presynaptic inputs did not improve the response rates (0.1 ms: $p = 0.761$, 0.2 ms: $p = 0.271$, 0.5 ms: $p = 0.810$). Thus, presynaptic inhibition did not play a significant role in suppressing the response rates. In all cases, we used stimulus amplitudes that evoked a spike in approximately 80% of the trials.

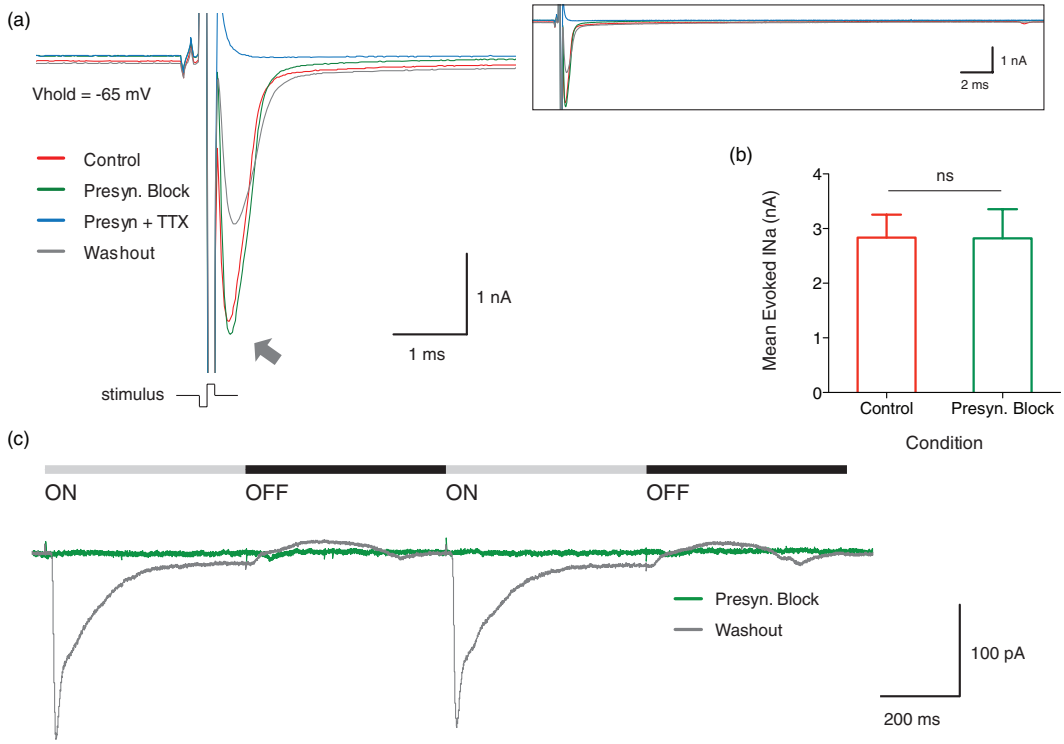

Figure 3. Evoking I_{Na} with extracellular electrical stimulation while voltage clamping RGCs at rest. (a) While clamping a RGC at rest, a 130 μA 0.1 ms extracellular pulse evoked a short-latency inward current (red, arrow), which was not an EPSC by its lack of sensitivity to presynaptic input blockers: CNQX + MK-801 + L-AP4 + pic + stry (green). But it was abolished by TTX (blue), suggesting voltage-gated sodium channels as the carrier. Washout partially reversed the effect of TTX (gray). All four traces were the average of ten repetitions. Inset: the same traces over a longer duration. (b) The amplitude of the inward current was not affected by presynaptic input blockers ($p = 0.3385$, repeated measure two-way ANOVA, $n = 3$ cells). (c) The effectiveness of the presynaptic input blockers was ascertained by the lack of light responses after wash in (green). Light-evoked responses were restored after washout (gray). Both traces were the average of five repetitions.

onset to the current peak) across the three cells were 2.83 ± 0.42 nA and 0.45 ± 0.003 ms, respectively. These characteristics are reminiscent of the sodium current responsible for action potentials. TTX, a potent and specific blocker for the voltage-gated sodium channels, completely eliminated the short-latency fast inward current in every case. This is demonstrated for one cell in figure 3(a) (blue trace). The block was partially reversed after washing out for 20 min in this example (gray trace). These observations suggest that the voltage-gated sodium channels were responsible for the inward currents, ruling out the possibility of oscillating stimulus artifacts or poorly compensated electrode and cell capacitive transients. Moreover, these inward currents always appeared as a single peak and were never followed by

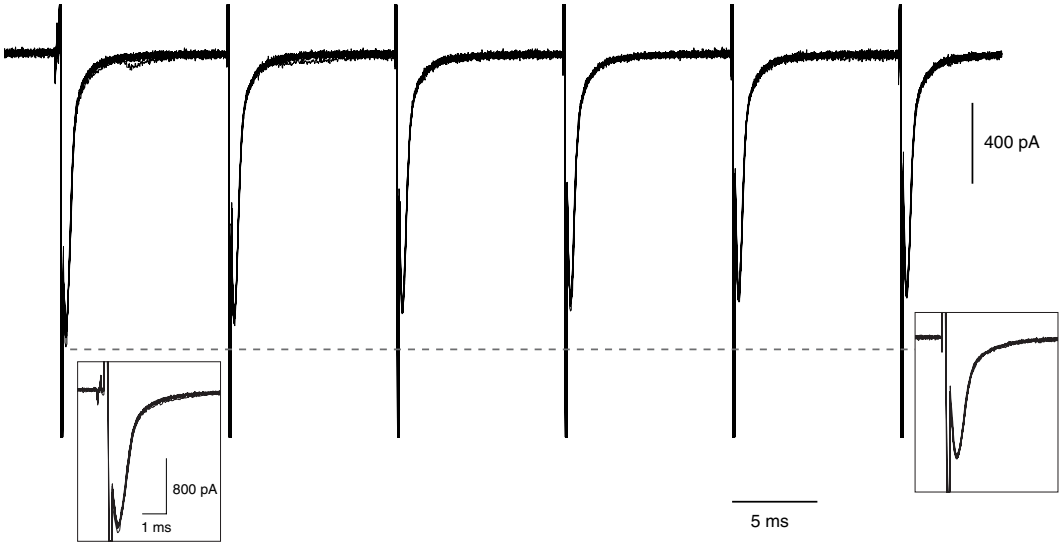

Figure 4. Measuring RGC I_{Na} evoked by repetitive extracellular electrical stimulation. Ten superimposed traces of a RGC stimulated with a 100 Hz train of six 110 μA 0.1 ms biphasic pulses. The electrically evoked I_{Na} was clearly separated from the stimulus artifacts (insets). The I_{Na} amplitude declined with repeated stimulation. This consistently occurred across all ten trials.

any outward current (figure 3(a) red, green and gray traces), which, had they occurred, would be indicative of insufficient voltage control and thus generation of action currents in unclamped regions.

We next ascertained that the inward currents were not due to EPSCs from retinal network activation. In each cell, we repeated the electrical stimulus while blocking all presynaptic inputs (CNQX + MK-801 + L-AP4 + pic + stry; figure 3(a), green trace). There was no significant difference in the evoked current amplitude before and during blocking across the three cells (figure 3(b); $p = 0.3385$, repeated measure two-way ANOVA), indicating that EPSC did not contribute to the short-latency fast inward current following electrical stimulation. Effective presynaptic input blocking was crucial for this reasoning. This was confirmed by the absence of light-evoked EPSC during drug perfusion (figure 3(c), green trace). The light-evoked EPSCs subsequently returned upon washout (figure 3(c), gray trace).

In summary, despite voltage clamping the RGCs near their resting potentials, extracellular electrical stimulation could activate the voltage-gated sodium channels, resulting in large-amplitude I_{Na} of several nA. In particular, the inward currents were not stimulus artifacts, uncompensated capacitive transients, artifacts of poor space clamp, nor EPSCs.

I_{Na} declines during repetitive stimulation

Because RGC I_{Na} could be evoked by extracellular stimulation while voltage clamping the cells at rest, we next used this technique to investigate the effect of repetitive stimulation on I_{Na}. Figure 4 shows ten superimposed current responses of a RGC stimulated with a train of six 0.1 ms pulses at 100 Hz ($V_{hold} = -65$ mV). The electrically evoked I_{Na} was apparent immediately following each stimulus artifact (figure 4 inset). A decline in the evoked I_{Na} peak, relative to the first response, was evident following the second stimulus, and by the sixth stimulus the evoked I_{Na} amplitude had fallen to $85.95 \pm 0.01\%$ relative to the first response.

Table 1. Fitting the decline of I_{Na} during repetitive stimulation with a one-phase exponential decay function.

Frequency (Hz)	α	K	SS	R^2
50	0.5043	0.2380	0.000 683	0.9922
100	0.3354	0.2382	0.006 171	0.9630
200	0.4152	0.6607	0.003 124	0.9867

The parameters α and k are the plateau limit and rate constant of the exponential decay function, respectively. The SS and R^2 values are the sum-of-squares and goodness-of-fit measures.

We quantified the change in evoked I_{Na} during repetitive direct stimulation with 16 RGCs (figure 5). Consistent with the observations in figure 4, the decline in relative I_{Na} following each pulse of the stimulus train was significant ($p < 0.0001$, two-way ANOVA) and also increased at higher stimulation frequencies ($p < 0.0001$). The relative I_{Na} for the 100 Hz stimuli (green) increased slightly at the end, from 0.54 ± 0.03 at the fifth pulse to 0.58 ± 0.03 at the sixth pulse. However, the difference was not significant (95% CI of difference $= -0.14$ to 0.06, Tukey's post-test). The decline in relative I_{Na} during repetitive stimulation was well described by an exponential decay function (figure 5(a), dotted lines). The parameters and goodness-of-fit values are listed in table 1. Since the short-latency stimulus-locked RGC spikes are due to activation of voltage-gated sodium channels (Sekirnjak *et al* 2006, Fried *et al* 2006), the declining I_{Na} should therefore influence RGC excitability during repetitive stimulation.

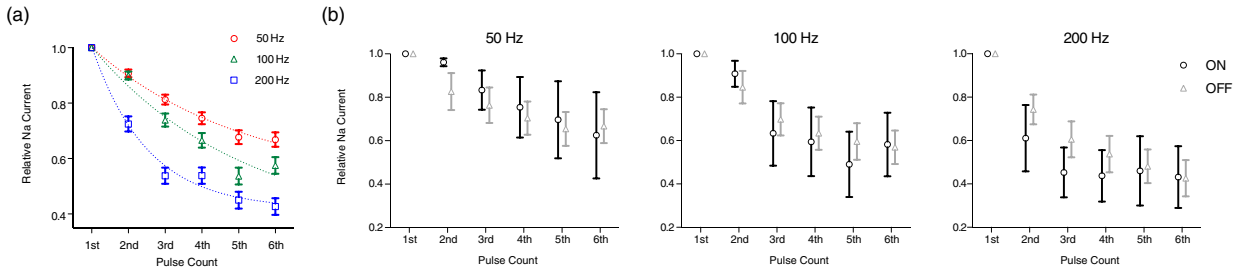

Figure 5. I_{Na} decline during repetitive stimulation of RGCs ($n = 16$) with 0.1 ms biphasic pulses. (a) The decline in relative I_{Na} was significant ($p < 0.0001$, two-way ANOVA). The decline also increased with higher stimulation frequencies ($p < 0.0001$). The dotted line for each frequency represents the one-phase exponential decay fit for the relative I_{Na} over the six pulses. (b) Comparison of relative I_{Na} between ON ($n = 5$) and OFF ($n = 8$) RGCs. The decline in relative I_{Na} between the pulses was significant (50 Hz: $p < 0.0019$, 100 Hz: $p < 0.0001$, 200 Hz: $p < 0.0001$), but there was no difference between the ON and OFF RGCs (50 Hz: $p = 0.4295$, 100 Hz: $p = 0.6762$, 200 Hz: $p = 0.2232$).

Comparison between ON and OFF cells

While several lines of evidence suggest that the behavioral differences between the ON and OFF RGCs may be largely determined by the afferent inputs they receive (Pang *et al* 2003, Murphy and Rieke 2006), Margolis and Detwiler (2007) recently reported intrinsic differences between ON and OFF alpha RGCs in mice (see also Myhr *et al* 2001, Margolis *et al* 2008, Sekirnjak *et al* 2011). To check if there are differences in I_{Na} decline rate between these two functionally distinct populations of RGCs following repetitive electrical stimulation, we compared their relative evoked I_{Na} (figure 5(b), from the same group of cells as figure 5(a), ON = 5 and OFF = 8). Consistent with the data from figure 5(a), the differences in relative I_{Na} between the pulses were significant (50 Hz: $p < 0.0019$, 100 Hz: $p < 0.0001$, 200 Hz: $p < 0.0001$) and increased with higher stimulation frequencies. There were more variations in the ON cell relative I_{Na}, possibly due to the smaller sample size. But we found no significant difference between these two classes across all three stimulation frequencies (50 Hz: $p = 0.4295$, 100 Hz: $p = 0.6762$, 200 Hz: $p = 0.2232$). Therefore, any differences between the ON and OFF cells did not have appreciable effects on the response rates of these cells during repetitive electrical stimulation, at least in the rabbit retina using the stimulus configurations tested here.

Increasing evoked I_{Na} prevents RGC spike response depression

A decline in I_{Na} during repetitive stimulation would reduce the RGCs' excitability, thus decreasing their response rate to repetitive stimulation. Notwithstanding this inference, as a further test, we reasoned that if I_{Na} reduction was the primary cause of RGC spiking response depression, then preventing I_{Na} decline during repetitive stimulation should prevent the decrease of the response rate. Instead of using fixed pulse amplitude, we scaled the pulse amplitude to progressively increase the driving force for I_{Na}. We derived the scaling factor (s_f) for each stimulus frequency by modifying the original one-phase exponential decay equation (see the methods section):

$$s_f = 1 + [1 - ((1 - \alpha) \times e^{-kn} + \alpha)].$$

For each frequency, we used the rate constant (k) and plateau limit (α) determined previously (table 1). The evoked I_{Na} is assumed to increase linearly with stimulus strength in this equation. Figure 6(a) illustrates the relative scaling of stimulus amplitude over the six repetitive pulses, after substituting k and α into the modified exponential equation. The scaling increased with stimulus frequency. For ease of discussion, we will refer to this procedure as 'adaptive current scaling' (ACS). When tested on four RGCs, the ACS stimulus trains improved the spiking response rate during repetitive stimulation compared to the control stimulus trains. This observation held for all frequencies (figure 6(b_1); 50 Hz: $p = 0.0004$, 100 Hz: $p = 0.0087$, 200 Hz: $p < 0.0001$, two-way ANOVA, $n = 4$). Furthermore, the differences in response rate between pulses in the ACS stimulus train were not significant (figure 6(b_1) green traces; 50 Hz: $p = 0.7040$, 100 Hz: $p = 0.8158$, 200 Hz: $p < 0.8771$, one-way ANOVA).

To quantify the effect of ACS on I_{Na}, we again measured the evoked I_{Na} during repetitive stimulation while voltage clamping the RGCs ($V_{hold} = -65$ mV). Comparing to the control pulse trains, the ACS pulse trains significantly increased the relative I_{Na} at all stimulation frequencies (figure 6(c_1); 50–200 Hz: $p < 0.0001$, two-way ANOVA, $n = 3$). With increasing stimulus frequencies, ACS began to overestimate the scaling required to counteract I_{Na} decline, as indicated by the relative I_{Na} values greater than unity (1.0). This is likely a consequence of the assumption that I_{Na} increases linearly with stimulus strength (see the discussion section). Nevertheless, these results strongly suggest that I_{Na} has a strong influence over RGC spiking response rate during repetitive stimulation. A decrease in evoked I_{Na} was associated with a decline in spiking response rate, while increasing the evoked I_{Na}, by applying progressively larger stimulus amplitudes, prevented the spiking response rate decline.

RGC intrinsic and light-evoked spiking frequencies

To ascertain that the stimulation frequencies used (50–200 Hz) were within the RGC physiological operating range, and importantly, that the response depression was not simply an artifact of our *ex vivo* experimental conditions; we examined

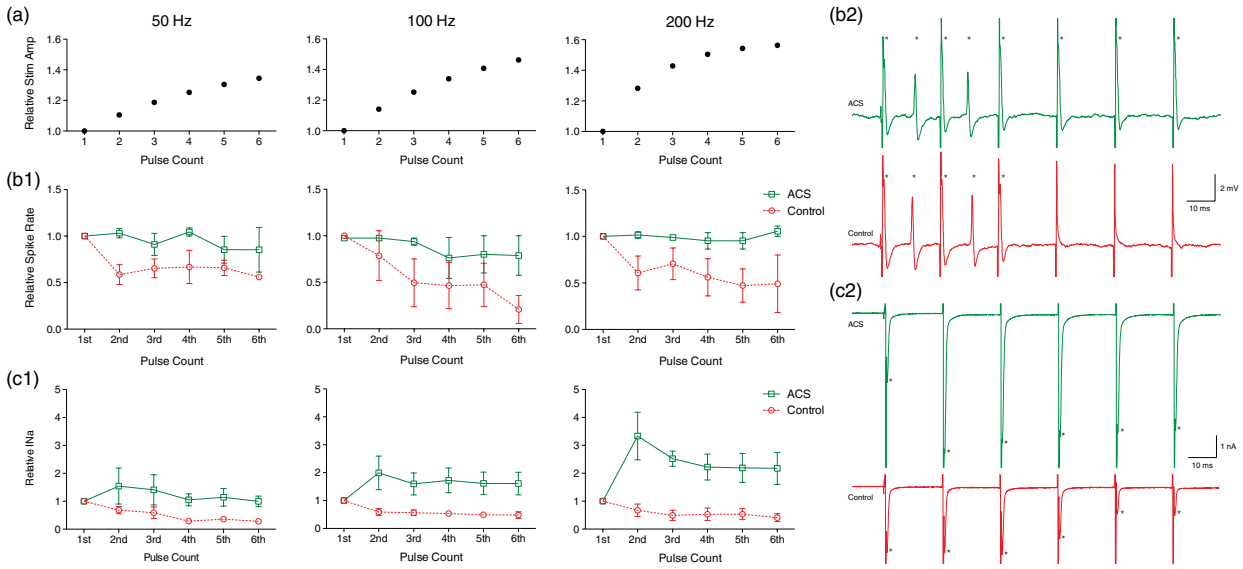

Figure 6. Increasing the evoked I_{Na} reduced spiking response depression. To facilitate comparison, all measurements were normalized relative to the response of the first stimulus. (a) Progressive increase in stimulus amplitude by ACS. (b_1) Comparing to the control, the spiking rates were increased by ACS (50 Hz: $p = 0.0004$, 100 Hz: $p = 0.0087$, 200 Hz: $p < 0.0001$, two-way ANOVA, $n = 4$ cells). The differences in response rates between the pulses in the ACS stimulus trains were insignificant (50 Hz: $p = 0.7040$, 100 Hz: $p = 0.8158$, 200 Hz: $p = 0.8771$, one-way ANOVA). As in figure 2, we used for the first pulse, stimulus amplitudes that evoked a spike in approximately 80% of trials. (b_2) Spiking responses (stars) of an RGC to a train of six 100 Hz pulses, with (green) and without (red) ACS. (c_1) ACS increased the relative I_{Na} when compared to control (50–200 Hz: $p < 0.0001$, two-way ANOVA, $n = 3$ cells). (c_2) Electrically evoked I_{Na} (marked by stars) of a RGC to six 100 Hz pulses with (green) and without (red) ACS.

the RGCs' ability to spike at high frequency using two techniques.

First we measured the ISIs evoked by injecting a 500 ms, 180 pA depolarizing pulse during current clamp. RGCs responded to the depolarization with a burst of action potentials. Consistent with previous findings (O'Brien *et al* 2002), almost all RGCs tested ($n = 43/49$) repeatedly fired action potentials during the entire depolarizing pulse (figure 7(a)). A few RGCs ($n = 6/49$) showed accommodation after a few spikes (figure 7(b)) and thus were unable to sustain repetitive spiking for prolonged periods. Nevertheless, to gain a quantitative measure of the firing frequencies across our RGC sample for comparison to repetitive electrical stimulation, we determined the duration of the first six ISIs during depolarizing pulse injection. When the cells were depolarized with a 180 pA pulse (figure 7(c)), the median durations (marked with 'x') of the first six ISIs ranged from 6.82 ms for the first ISI to 14.34 ms for the last ISI. These values correspond to spiking frequencies 70–147 Hz. To examine the effects of depolarization amplitude, we tested stronger depolarization at 320 pA ($n = 26$ cells). The durations of the first six ISIs decreased with stronger depolarization. The median duration for the first ISI was 5.17 ms and 10.27 ms by the sixth ISI (figure 7(d)), corresponding to spiking frequencies 97–193 Hz.

While RGCs were generally capable of repetitive firing at 50–200 Hz upon depolarization by intracellular current injection, the ISI durations were pulse-strength dependent. Thus, the question arises whether the depolarizing pulse we injected was physiologically relevant, since under normal conditions RGC ISIs not only depend on their intrinsic properties but also on the properties and connections of the presynaptic pathway. Therefore, we next measured the RGC ISIs during light stimulation.

In figure 8(a), an RGC fired a volley of action potentials in response to a 1 s light stimulus (first sweep in black). The spikes from all repetitions are plotted together in the raster plot below the membrane potential traces. We presented the light stimuli to 45 RGCs. The ISIs were strongly biased toward short durations (figure 8(b)), and could be as short as 2 ms throughout the first six ISIs. To more precisely quantify the ISIs, we fitted the distribution for the first six ISIs with a log-normal PDF and calculated the mode for each ISI. The mode (marked with 'x' in figure 8(b)) was lowest for the first ISI at 4.20 ms and highest at 5.22 ms for the sixth ISI. These modes approximately correspond to spiking frequencies of 192–238 Hz. To provide an indication for the spikes elicited by the 1 s light stimulus in these RGCs, we also plotted the elicitation probability for the first six ISIs (figure 8(c)). The probability of having the fifth spike was 0.688. Therefore, 68.8% of the cells spiked at least six times when stimulated by the light for 1 s.

In summary, we evaluated the RGCs' ability to spike at high frequencies with two complementary techniques. Despite some variability from cell to cell, possibly due to variations between different RGC classes, most cells were intrinsically capable of high-frequency spiking for several consecutive spikes and did so when driven by light stimuli. Therefore, the response depression observed during repetitive extracellular stimulation at 50–200 Hz was unlikely to be an artifact of the

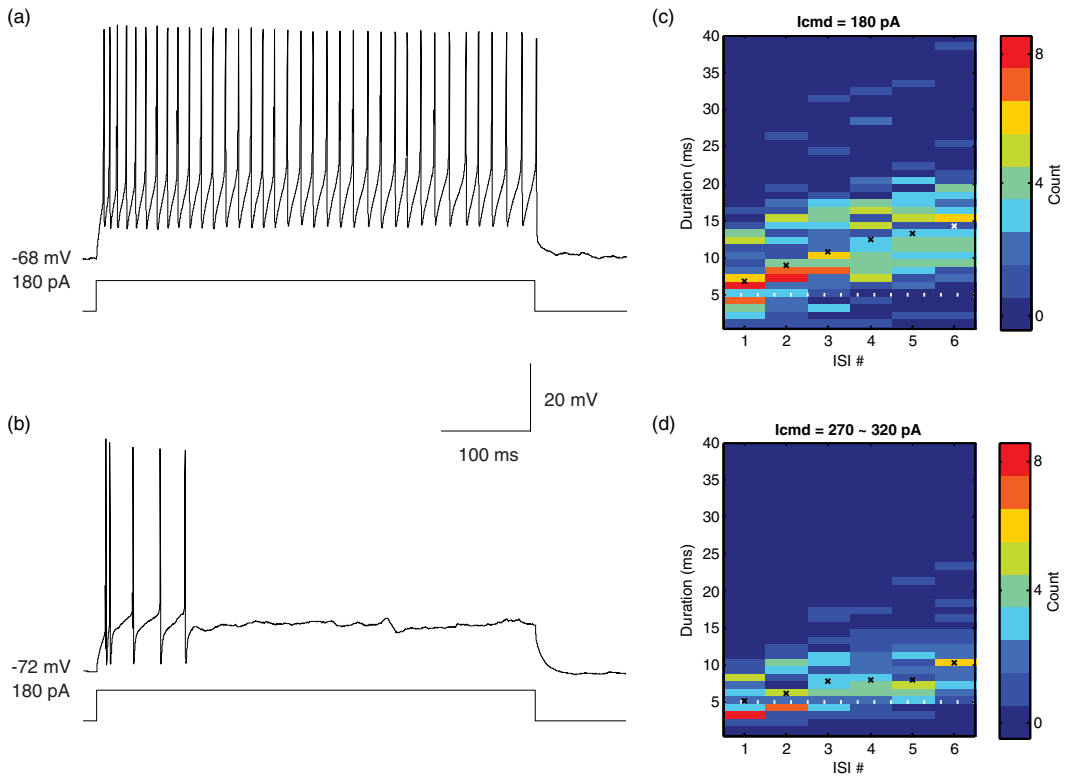

Figure 7. RGC ISIs during depolarizing pulse injection. (a) Most RGCs ($n = 43/49$) spiked continuously throughout the duration of the 180 pA depolarizing pulse. (b) A small number of cells ($n = 6/49$) showed spike accommodation. (c) Duration distribution summary of the first six ISIs of 49 RGCs to 180 pA pulse injection. The median duration for each ISI (marked by 'x') ranged from 6.82 ms for the first ISI to 14.34 ms by the last ISI. The dashed line designates the 5 ms time point. (d) Duration distribution summary for 26 of the 49 RGCs, where we also tested 320 pA pulse injection. The medians decreased to 5.17 and 10.27 ms for the first and last ISI, respectively.

ex vivo conditions. Failure of electrical stimulation to reliably elicit spikes at similar frequencies may thus have important consequences on the perceptual efficacy of electrically evoked percepts.

Discussion

We showed that the spiking response depression of directly activated RGCs during electrical stimulation was not mediated by retinal network inhibition. Instead, I_{Na} played a key role in determining RGC spiking probability. Under identical conditions, RGCs were intrinsically capable of high-frequency spiking and did so when driven by light. A decline in I_{Na} was associated with decreasing RGC spiking response rate. Conversely, counteracting the I_{Na} decline with progressively stronger stimuli prevented the response depression.

Underlying causes for I_{Na} decline

In this study, we demonstrated a causal relationship between I_{Na} decline and spiking response depression. The question thus arises regarding the underlying mechanisms responsible for the electrically evoked decline of I_{Na}. The RGC axon initial segment (AIS) contains a high density of Na_v 1.6 and Na_v 1.2 sodium channel subtypes (Lai and Jan 2006), which are thought to be responsible for action potential initiation (Kole *et al* 2008, Hu *et al* 2009). This site also has the lowest threshold for spike generation during extracellular electrical stimulation (Fried *et al* 2009; see also Jensen *et al* 2003; Sekirnjak *et al* 2008). Therefore, these two sodium channel subtypes likely play a critical role in determining RGC electrically evoked responses. The present results are consistent with previous findings of sodium channel inactivation following repeated depolarization (Bishop *et al* 1959, Sefton and Swinburn 1964, Tsutsui and Oka 2002, Debanne 2004). To avoid these conditions, retinal implants may need to adopt a stimulation strategy consisting of brief stimulus bursts interleaved by periods of inactivity, a pattern akin to light-evoked RGC responses under physiological conditions (Meister 1999).

I_{Na} inactivation may not be the only mechanism responsible for spiking response depression. Some factors implicated in use-dependent failure of axonal spikes and action potential propagation include activity-dependent hyperpolarization by calcium-mediated potassium conductance ($I_{K(Ca)}$; Bielefeldt and Jackson 1993), extracellular potassium accumulation following repeated depolarization (Grossman *et al* 1979) and modulation by the hyperpolarization-activated non-selective cationic current

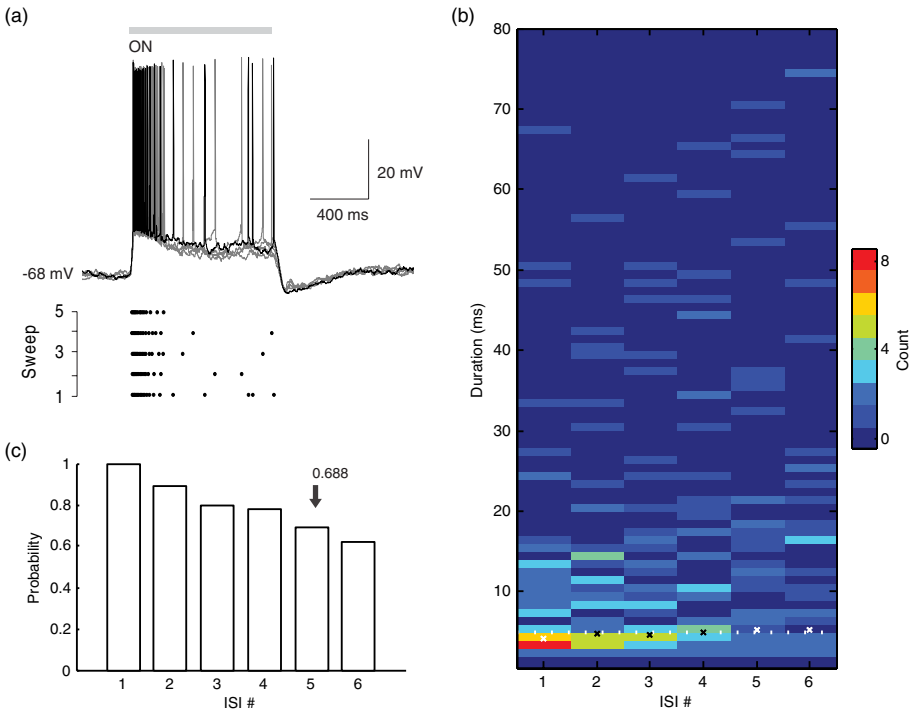

Figure 8. RGC ISIs during 1 s light stimulation. (a) Five superimposed responses of an ON-type RGC. The cell fired a train of action potentials on a sustained depolarization. The first trial is in black. The raster plot (below) shows the spike times for all five trials. (b) Duration distribution for the first six ISIs of 45 RGCs to light stimulation. The mode (marked by 'x') ranged from 4.20 ms for the first ISI to 5.22 ms for the sixth ISI. The dashed line designates the 5 ms time point. (c) The elicitation probability of the first six ISIs for the RGCs in (b), 68.8% of the cells spiked at least six times when stimulated by the light.

(I_h; Soleng *et al* 2003). Since the AIS, and thus more generally the axon, is targeted by electrical stimulation, these factors, if present in RGC axons, could also contribute to the response depression observed.

Spiking response depression during repetitive stimulation—does it matter?

Some RGCs may be inherently unable to spike repetitively at high frequencies. During intracellular depolarizing current injection, accommodation occurred after a few spikes in a small number ($n = 6/49$) of cells. It would be inappropriate to expect these cells to follow high-frequency electrical stimulation beyond a few pulses. While we did not morphologically identify these cells, the spiking patterns (figure 7(b)) were very similar to the theta cells in O'Brien *et al* (2002). Nevertheless, consistent with previous reports (Berry and Meister 1998, Zeck and Masland 2007), most RGCs (∼88%) were intrinsically capable of high-frequency spiking when presented with appropriately strong stimuli. Given the high temporal precision and trial-to-trial reproducibility of light-evoked RGC spikes (Meister and Berry 1999, Baccus 2007, Gollisch and Meister 2010), a reduction in spike elicitation reliability during repetitive electrical stimulation will likely have important ramifications for the perceptual efficacy of retinal prostheses.

Why does prosthetic stimulation appear less effective than light at driving high-frequency spikes?

As a mechanism intrinsic to RGCs, the declining I_{Na} would affect light-evoked responses as much as electrically evoked responses. Why then are the cells able to fire reliably at high frequencies (50–200 Hz) for several spikes or more during light stimulation (figure 8), while extracellular electrically evoked responses showed an immediate decline in spiking probability at stimulation frequency as low as 50 Hz? Two observations could reconcile this disparity. First, there are mechanistic differences between light-evoked and electrically evoked RGC responses. Light stimuli activate (in the following order) the ligand-gated currents, the voltage-gated currents and finally sodium spikes at the AIS. Activating the ligand-gated and the voltage-gated currents could result in sustained depolarization, for instance, by virtue of the NMDA receptors (Copenhagen 2003) and L-type calcium channels (Ishida 2003) present in RGCs, respectively. This sustained depolarization plateau (see figure 8(a)) could provide sufficient drive for repeated spike generation even in the presence of gradual I_{Na} inactivation, a situation similar to repeated spiking through depolarizing current injection (figure 7). In contrast, electrical stimulation of RGCs recruits the I_{Na} directly (Fried *et al* 2006, Sekirnjak *et al* 2006), bypassing the ligand-gated currents entirely. The sustained voltage-gated currents, with slower activation kinetics than I_{Na}, may be poorly recruited by the short-duration (0.1–0.5 ms) biphasic pulses. The lack of sustained

depolarization thus comparatively decreases the excitability of RGCs, especially with concomitant I_{Na} inactivation. Second, it is worthwhile comparing the definition of threshold for light-evoked and electrically evoked responses. In the period following a visual event in which a RGC fires a burst of action potentials, the EPSP is sufficiently powerful and sustained to ensure high-frequency spiking. However, the definition of threshold for electrical stimulation is typically defined as the current amplitude that elicits spike(s) in some percentage of the trials (often 50%). This definition, in effect, sets a low safety margin for spike elicitation in the presence of I_{Na} inactivation.

Given prior studies with similar conclusions (e.g. Sekirnjak *et al* 2006, Tsai *et al* 2009), it seems unlikely that the stimulation configuration was responsible for the response depression. For instance, Sekirnjak and colleagues used epiretinal stimulation with pulse configurations different from the present study, and in a previous study, we used a single monopolar electrode rather than a multielectrode array. Furthermore, a range of species have been used across these studies (rabbits, mice, rat and primates).

Preventing RGC spiking response depression

The present ACS implementation assumed the evoked I_{Na} to scale linearly with stimulus amplitude. Two observations suggest that this approximation overestimated the stimulus increase needed for counteracting I_{Na} decline. First, as we increased the scaling factor with stimulus frequency, it was evident in figure 6(c) that the relative differences in evoked I_{Na} between the control pulse trains and the ACS pulse trains also increased. Second, previous reports have found RGC spike elicitation probability to scale in a sigmoidal fashion with stimulus amplitude (Sekirnjak *et al* 2006, Tsai *et al* 2009, Fried *et al* 2009). Indeed, the I_{Na} voltage-dependent activation and inactivation kinetics are well described by the Boltzmann equation, not the linearity assumed in the modified one-phase exponential equation. ACS prevented the response depression in the isolated retina. A similar methodology may be useful for preventing fading responses in clinical applications. While the overestimation here is inconsequential for demonstrating the role of I_{Na} in RGC response depression, stimulus amplitude overestimation in clinical applications does reduce the safety margin to the electrode charge injection limit, which if exceeded, will reduce the electrode lifetime (Merrill *et al* 2005). In this study, we determined the scaling function at fixed stimulation frequencies. Retinal implants will likely need dynamically changing stimulation frequencies, as determined by the visual inputs. Further work will be necessary to derive the general form for the scaling function under such conditions.

The causes of fading percepts in human subjects are likely multifaceted. In a small number of patients, percepts disappeared in less than a second when stimulating at greater than a few Hz (Christopher *et al* 2010, Zrenner *et al* 2010). The findings made in the isolated retinal studies, where RGC spiking response rate declined when stimulating at >50 Hz, do not account for the severe fading in these individuals. Additional factors such as the degenerate retina and visual cortical activities may have added further complexities to the issue.

Comparison to recent reports

There are conflicting reports regarding the extent to which RGCs could follow high-frequency extracellular pulse trains (Sekirnjak *et al* 2006, Tsai *et al* 2009, Ahuja *et al* 2008). In an attempt to reconcile these discrepancies, a recent report by Cai *et al* (2011) found that, using extracellular recordings, when a pulse in a high-frequency stimulus train failed to elicit an action potential, a small-amplitude biphasic response was often observed. If these small-amplitude responses were included, then some RGCs could follow stimulus rates up to 600 Hz. These small-amplitude responses are likely the spikelets we observed during whole-cell patch recordings (figure 1(c)). These spikelets are presumably the AIS spikes that failed to result in full action potentials (Cai *et al* 2011, Hu *et al* 2009). The ability of RGCs to following high-frequency pulse trains ultimately depends on the responses, whether full action potentials or spikelets, propagating down the axon to higher visual centers. It is not clear if the spikelets could do so successfully, because they are not observed following light stimulation or intracellular depolarizing pulse injection. Nonetheless, the ACS technique presented here could be used to circumvent potential spikelet propagation failures by eliciting full RGC action potentials instead.

Acknowledgments

We thank Professor William R Levick (Australian National University) for discussion. This research was supported in part by an Australian Research Council Special Research Initiative in Bionic Vision Technologies.

References

Ahuja A K, Behrend M R, Kuroda M, Humayun M S and Weiland J D 2008 An *in vitro* model of a retinal prosthesis *IEEE Trans. Biomed. Eng.* **55** 1744–53

Baccus S A 2007 Timing and computation in inner retinal circuitry *Annu. Rev. Physiol.* **69** 217–90

Berry M J and Meister M 1998 Refractoriness and neural precision *J. Neurosci.* **18** 2200–11

Berry M J, Warland D K and Meister M 1997 The structure and precision of retinal spike trains *Proc. Natl Acad. Sci. USA* **94** 5411–16

Bielefeldt K and Jackson M B 1993 A calcium-activated potassium channel causes frequency-dependent action-potential failures in a mammalian nerve terminal *J. Neurophysiol.* **70** 284–98

Bishop P O, Burke W and Hayhow W R 1959 Repetitive stimulation of optic nerve and lateral geniculate synapses *Exp. Neurol.* **1** 534–55

Cai C, Ren Q, Desai N, Rizzo J and Fried S 2011 Response variability to high rates of electric stimulation in retinal ganglion cells *J. Neurophysiol.* **106** 153–62

Christopher P, McMahon M J, Patel U, Wei J, Greenberg R J and Dorn J D 2010 The temporal dynamics of percepts generated by the ArgusTM II epiretinal prosthesis *Neuroscience Meeting Planner, Program no 20.3 2010* (San Diego, CA: Society for Neuroscience) online

Copenhagen D 2003 Excitation in retina: the flow, filtering, and molecules of visual signalling in the glutamatergic pathways from photoreceptors to ganglion cells *The Visual Neurosciences* ed L M Chalupa and J S Werner (Cambridge, MA: MIT Press)

Debanne D 2004 Information processing in the axon *Nat. Rev. Neurosci*. **5** 304–16
Freeman D K and Fried S I 2011 Multiple components of ganglion cell desensitization in response to prosthetic stimulation *J. Neural Eng*. **8** 016008
Fried S I, Hsueh H A and Werblin F S 2006 A method for generating precise temporal patterns of retinal spiking using prosthetic stimulation *J. Neurophysiol*. **95** 970–8
Fried S I, Lasker A C W, Desai N J, Eddington D K and Rizzo J F III 2009 Axonal sodium channel bands shape the response to electric stimulation in retinal ganglion cells *J. Neurophysiol*. **101** 1972–87
Fujikado T *et al* 2007 Evaluation of phosphenes elicited by extraocular stimulation in normals and by suprachoroidal-transretinal stimulation in patients with retinitis pigmentosa *Graefes Arch. Clin. Exp. Ophthalmol*. **245** 1411–9
Gekeler F, Messias A, Ottinger M, Bartz-Schmidt K U and Zrenner E 2006 Phosphenes electrically evoked with DTL electrodes: a study in patients with retinitis pigmentosa, glaucoma, and homonymous visual field loss and normal subjects *Invest. Ophthalmol. Vis. Sci*. **47** 4966–74
Gerding H, Eckmiller R E, Hornig R, Ortmann V, Kolck A and Taneri S 2002 Safety assessment and acute clinical tests of epiretinal retina implants *Invest. Ophthalmol. Vis. Sci*. **43** 4488 (E-Abstract)
Gollisch T and Meister M 2010 Eye smarter than scientists believed: neural computations in circuits of the retina *Neuron* **65** 150–64
Greenwald S H, Horsager A, Humayun M S, Greenberg R J, McMahon M J and Fine I 2009 Brightness as a function of current amplitude in human retinal electrical stimulation *Invest. Ophthalmol. Vis. Sci*. **50** 5017–25
Grossman Y, Parnas I and Spira M 1979 Ionic mechanisms involved in differential conduction of action potentials at high frequency in a branching axon *J. Physiol*. **295** 307–22
Horsager A, Boynton G M, Greenberg R J and Fine I 2011 Temporal interactions during paired-electrode stimulation in two retinal prosthesis subjects *Invest. Ophthalmol. Vis. Sci*. **52** 549–57
Hu W, Tian C, Li T, Yang M, Hou H and Shu Y 2009 Distinct contributions of Nav1.6 and Nav1.2 in action potential initiation and backpropagation *Nat. Neurosci*. **12** 996–1004
Ishida A T 2003 Retinal ganglion cell excitability *The Visual Neurosciences* ed L M Chalupa and J S Werner (Cambridge, MA: MIT Press)
Jensen R J and Rizzo J F III 2007 Responses of ganglion cells to repetitive electrical stimulation of the retina *J. Neural Eng*. **4** 1–6
Jensen R J, Rizzo J F, Ziv O R, Grumet A and Wyatt J 2003 Thresholds for activation of rabbit retinal ganglion cells with an ultrafine, extracellular microelectrode *Invest. Ophthalmol. Vis. Sci*. **44** 3533–43
Kole M H P, Ilschner S U, Kampa B M, Williams S R, Ruben P C and Stuart G J 2008 Action potential generation requires a high sodium channel density in the axon initial segment *Nat. Neurosci*. **11** 178–86
Lai H C and Jan L Y 2006 The distribution and targeting of neuronal voltage-gated ion channels *Nat. Rev. Neurosci*. **7** 548–62
Llinas R, Baker R and Sotelo C 1974 Electrotonic coupling between neurons in cat inferior olive *J. Neurophysiol*. **37** 560–71
Margalit E and Thoreson W B 2006 Inner retinal mechanisms engaged by retinal electrical stimulation *Invest. Ophthalmol. Vis. Sci*. **47** 2606–12
Margolis D J and Detwiler P B 2007 Different mechanisms generate maintained activity in ON and OFF retinal ganglion cells *J. Neurosci*. **27** 5994–6005
Margolis D J, Newkirk G, Euler T and Detwiler P B 2008 Functional stability of retinal ganglion cells after degeneration-induced changes in synaptic input *J. Neurosci*. **2008** 6526–36
Meister M and Berry M J 1999 The neural code of the retina *Neuron* **22** 435–50
Merrill D R, Bikson M and Jefferys J G R 2005 Electrical stimulation of excitable tissue: design of efficacious and safe protocols *J. Neurosci. Methods* **141** 171–98
Murphy G J and Rieke F 2006 Network variability limits stimulus-evoked spike timing precision in retinal ganglion cells *Neuron* **52** 511–24
Myhr K L, Lukasiewicz P D and Wong R O L 2001 Mechanisms underlying developmental changes in the firing patterns of ON and OFF retinal ganglion cells during refinement of their central projections *J. Neurosci*. **21** 8664–71
O'Brien B J, Isayama T, Richardson R and Berson D M 2002 Intrinsic physiological properties of cat retinal ganglion cells *J. Physiol*. **538** 787–802
Pang J J, Gao F and Wu S M 2003 Light-evoked excitatory and inhibitory synaptic inputs to ON and OFF α ganglion cells in the mouse retina *J. Neurosci*. **22** 6063—73
Rizzo J F, Jensen R J, Loewenstein J and Wyatt J 2003 Methods and perceptual thresholds for short-term electrical stimulation of human retina with microelectrode arrays *Invest. Ophthalmol. Vis. Sci*. **44** 5355–61
Sefton A J and Swinburn M 1964 Electrical activity of lateral geniculate nucleus and optic tract of the rat *Vision Res*. **4** 315–28
Sekirnjak C, Hottowy P, Sher A, Dabrowski W, Litke A M and Chichilnisky E J 2006 Electrical stimulation of mammalian retinal ganglion cells with multielectrode arrays *J. Neurophysiol*. **95** 3311–27
Sekirnjak C, Hottowy P, Sher A, Dabrowski W, Litke A M and Chichilnisky E J 2008 High-resolution electrical stimulation of primate retina for epiretinal implant design *J. Neurosci*. **28** 4446–56
Sekirnjak C, Jepson L H, Hottowy P, Sher A, Dabrowski W, Litke A M and Chichilnisky E J 2011 Changes in physiological properties of rat ganglion cells during retinal degeneration *J. Neurophysiol*. **2011** 2560–71
Soleng A, Chiu K and Raastad M 2003 Unmyelinated axons in the rat hippocampus hyperpolarize and activate an H current when spike frequency exceeds 1 Hz *J. Physiol*. **552** 459–70
Spencer W A and Kandel E R 1961 Electrophysiology of hippocampal neurons: IV. Fast prepotentials *J. Neurophysiol*. **24** 272–85
Stephens M A 1974 EDF statistics for goodness of fit and some comparisons *J. Am. Stat. Assoc*. **69** 730–7
Tsai D, Morley J W, Suaning G J and Lovell N H 2009 Direct activation and temporal response properties of rabbit retinal ganglion cells following subretinal stimulation *J. Neurophysiol*. **102** 2982–93
Tsutsui H and Oka Y 2002 Slow removal of Na+ channel inactivation underlies the temporal filtering property in the teleost thalamic neurons *J. Physiol*. **539** 743–53
Vaney D 1980 A quantitative comparison between the ganglion cell populations and axonal outflows of the visual streak and periphery of the rabbit retina *J. Comp. Neurol*. **189** 215–33
Zeck G M and Masland R H 2007 Spike train signatures of retinal ganglion cell types *Eur. J. Neurosci*. **26** 367–80
Zheng J-J, Lee S and Zhou Z J 2004 A developmental switch in the excitability and function of the starburst network in the mammalian retina *Neuron* **44** 851–64
Zhou Z J and Fain G L 1996 Starburst amacrine cells change from spiking to nonspiking neurons during retinal development *Proc. Natl Acad. Sci. USA* **1996** 8057–62
Zrenner E, Benav H, Bruckmann A, Greppmaier U, Kusnyerik A, Stett A, Stingl K and Wilke R 2010 Electronic implants provide continuous stable percepts in blind volunteers only if the image receiver is directly linked to eye movement *2010 ARVO Meeting Planner, Program no 444* (Fort Lauderdale, FL: ARVO) (online)